COMPARATIVE ANALYSIS OF NON-METALLIC INCLUSIONS IN LASER-WELDED CP AND TRIP STEELS

KOZŁOWSKA Aleksandra[1], GRZEGORCZYK Barbara[1], KAMIŃSKA Małogorzata[2], RÓŻAŃSKI Maciej[3]

[1] *Institute of Engineering Materials and Biomaterials, Silesian University of Technology, Gliwice, Poland, EU,* aleksandra.kozlowska@polsl.pl, barbara.grzegorczyk@polsl.pl

[2] *Institute of Non-Ferrous Metals, Gliwice, Poland, EU,* malgorzata.kaminska@imn.gliwice.pl

[3] *Institute of Welding, Gliwice, Poland, EU,* maciej.rozanski@is.gliwice.pl

Abstract

In this study, the quantity, size and type of non-metallic inclusions occurring in laser welded transformation induced plasticity (TRIP) and complex phase (CP) steel joints were identified using SEM and EDS techniques. Both steels include Al, Ti, and Si additions which are characterized by high chemical affinity to oxygen. Microscopic observations of the fusion zones of the TRIP and CP steels showed that the quantity and size of inclusions formed in the CP steel were significantly lower than those observed in the fusion zone of TRIP steel. The presence of oxide-type non-metallic inclusions containing Al, Ti and Si has been primarily revealed.

Keywords: AHSS, TRIP steel, CP steel, non-metallic inclusions, laser welding

1. INTRODUCTION

The results of research in field of materials science have a significant impact on the development of modern materials used as components of the car's body. Today, steels are still the main constructional materials used in the automotive industry. However, conventional steel grades are increasingly replaced by newer types of high strength steels. Modern steels are characterized by a multiphase structure which provides good mechanical and technological properties [1, 2]. First generation of AHSS (Advanced High Strength Steels) includes transformation induced plasticity (TRIP) and complex phase (CP) steels, which are characterized by effective combination of high strength and plasticity. Moreover, these materials are able to absorb energy under the dynamic deformation conditions - during a crash event. The combination of mechanical properties depends on many factors, such as chemical composition, heat treatment and metallurgical cleanliness of steel related to the amount of non-metallic inclusions [3-7]. Generally, non-metallic inclusions are considered to deteriorate the toughness, ductility, fatigue strength and corrosion resistance of steel. Presence of non-metallic inclusions can lead to the premature destruction of elements due to the occurrence of cracks at a location of particles [8, 9]. TRIP and CP steels include Al, Ti, and Si additions which form different types of sulfides, oxides or more complex inclusions.

Resistance spot welding is a commonly used method of joining parts of car's components. Despite many advantages such as high efficiency, resistance welding is increasingly replaced by laser welding, characterized by high power density, high process flexibility and high welding rate with small distortion of elements being welded [10-14]. It is well known that welding conditions affect the chemical composition and microstructure of steel joints. Therefore, the objective of the present study was to identify the type, size and amount of non-metallic inclusions formed in the fusion zone of TRIP and CP steel joints.

2. EXPERIMENTAL PROCEDURE

The investigated materials were TRIP and CP steels with the chemical composition shown in **Table 1**. The TRIP steel ingots were prepared using a vacuum-induction furnace (under Ar atmosphere), subsequently hotforged and roughly rolled to a thickness of about 5 mm. Samples of 2 mm in thickness for welding purposes were obtained after thermomechanical rolling and controlled cooling. Samples of CP steel were prepared form the commercial thermomechanically rolled CPW 800 steel sheet (thickness of about 2.5 mm). The laser welding processes were carried out in an air atmosphere using the keyhole welding technique with a solid-state laser TruDisk 12002 type Yb:YAG integrated with a robotized laser treatment system [15]. Heat input value of 0.05 kJ / mm was applied. Fusion zones of TRIP and CP steel welds were examined using optical microscopy (Zeiss Axio Observer Z1m optical microscope). Two groups of specimens were examined: polished samples - in order to reveal non-metallic inclusions occurring in a fusion zone, and etched samples - prepared using 5 % nital in order to reveal the microstructure. Morphological details of microstructures and chemical composition of non-metallic inclusions were characterized by scanning electron microscope (SEM, Zeiss SUPRA 25) using EDS-technique. The point analyses and EDS-mapping were carried out.

Table 1 Chemical composition of the investigated steels (wt. %)

Steel grade	C	Mn	Si	Al	Cr	Nb	Ti	Mo	S	P	N
TRIP	0.24	1.55	0.87	0.40	-	0.034	0.023	-	0.004	0.010	0.0028
CPW 800	0.08	1.72	0.56	0.29	0.34	0.005	0.125	0.016	0.003	0.010	0.0020

3. RESULTS AND DISCUSSION

Morphology of the individual microstructural constituents present in the base material was identified using scanning electron microscopy (SEM). The micrograph in **Figure 1a** shows the microstructure of the TRIP steel base material. The multiphase structure is composed of fine-grained ferrite, bainite and retained austenite. Individual grains of retained austenite are located at ferrite boundaries. Moreover, the presence of interlath retained austenite located in bainitic regions was identified. A small fraction of austenite transformed into martensite upon cooling forming martensite-austenite (M-A) constituents. A base material of CP steel contains fine-grained ferrite-bainite matrix with the martensite-austenite (M-A) islands. Additionally, the presence of small retained austenite grains was observed (**Figure 1b**).

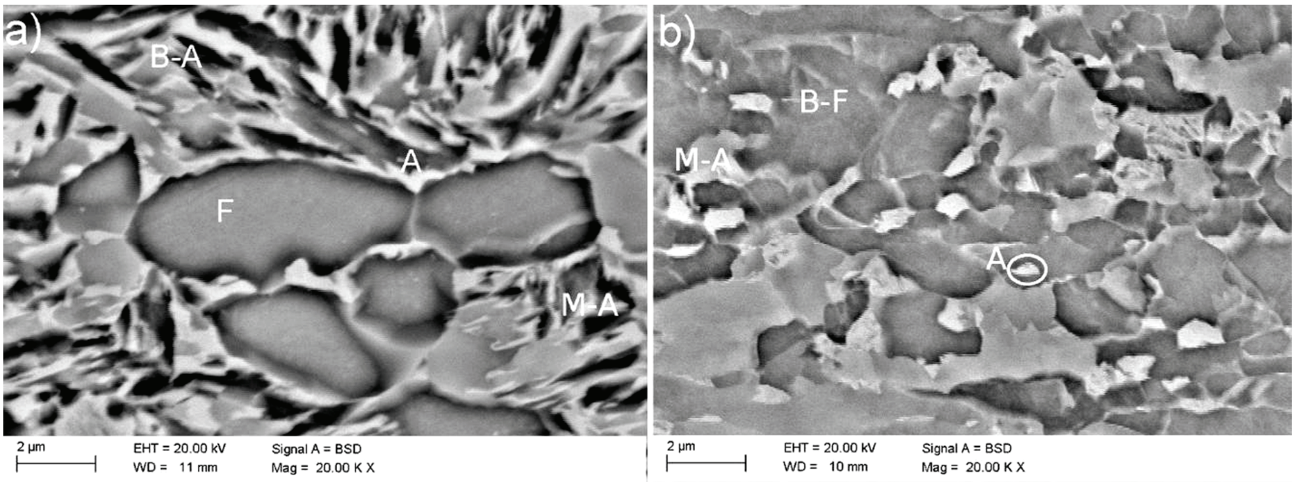

Figure 1 Microstructure of the base metal: a) TRIP steel, b) CP steel

Microscopic observations of the laser-welded polished samples (**Figure 2a** and **Figure 2b**) indicate that both investigated steels possess some fraction of non-metallic inclusions located mainly in the fusion zone (FZ) of the weld. It can be seen that the amount of inclusions in the heat affected zone is significantly smaller - a clear boundary between the fusion zone and heat affected zone can be observed. The distribution of particles in the FZ is quite uniform. Detailed information about the microstructure and morphology of non-metallic inclusions present in the fusion zone of investigated steels were determined using scanning electron microscope. SEM image of the TRIP steel (**Figure 3a**) shows the microstructure of the FZ composed of columnar crystals of lath morphology with some fraction of interlath retained austenite. Laser welding caused the changes of the multiphase structure of steel, i.e., the heat input to the material in combination with a fast cooling rate lead to creation of martensitic-bainitic laths [14-16]. Moreover, a large number of globular inclusions characterized by various size located in martensitic-bainitic regions were observed. The microstructure of FZ of the CP steel is composed of martensite laths and isolated, globular inclusions with a very small diameter (**Figure 3b**). In comparison to the TRIP steel, a significant reduction of the amount of inclusions distributed in FZ was observed.

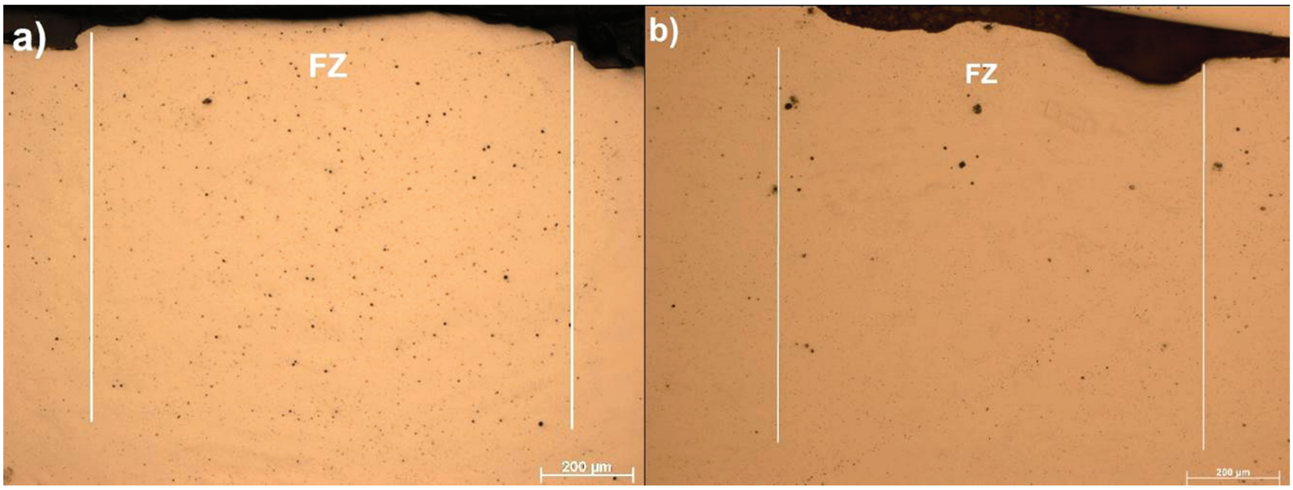

Figure 2 Distribution of non-metallic inclusions in the fusion zone (FZ): a) TRIP steel, b) CP steel; polished samples

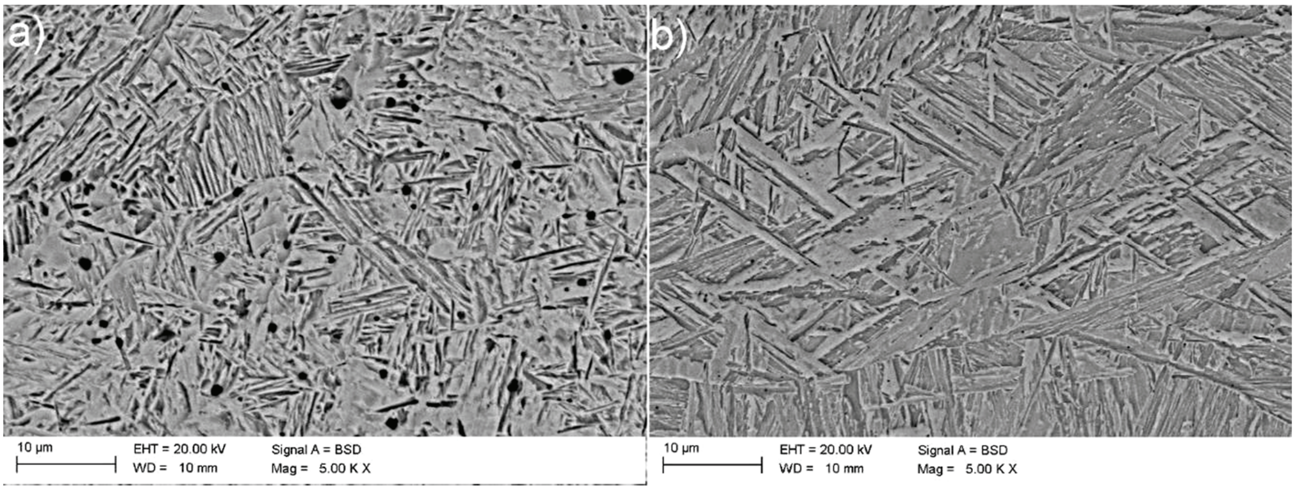

Figure 3 SEM micrographs of the non-metallic inclusions in the fusion zone (FZ): a) TRIP steel, b) CP steel

Appearance of non-metallic inclusions is related to the conditions of welding process. Lack of the protecting atmosphere and the presence of elements with the strong chemical affinity to oxygen (Al, Mn, Si) in the investigated steels are reflected by the increased quantity of oxide-type inclusions observed in the FZ. **Figure 4** presents non-metallic inclusions of various sizes distributed in the FZ of TRIP steel. The particles are located at the martensitic-bainitic laths. Chemical analysis of the individual inclusion (**Figure 4b**) showed high content of oxygen, aluminium, manganese and silicon. It shows that a complex oxide containing Al, Mn, Si was formed. The content of Al in the inclusion is much higher when compared to Si and Mn. It is caused by higher chemical affinity of Al to oxygen.

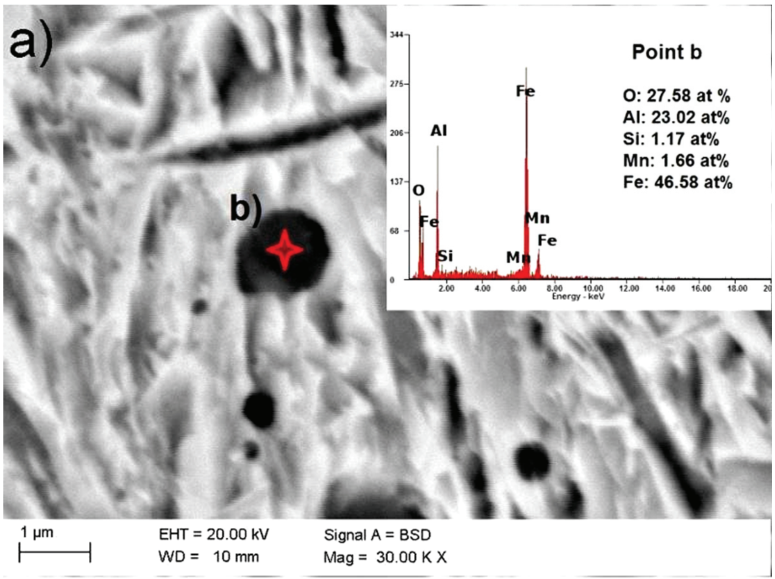

Figure 4 Non-metallic inclusions detected in the fusion zone of TRIP steel (a); EDS analysis of particle from point marked as b (b)

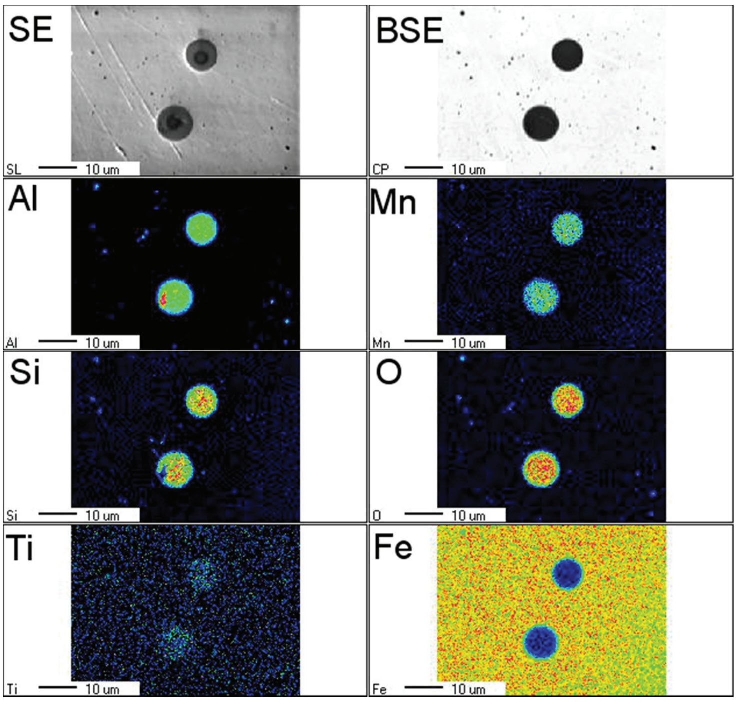

Figure 5 Elemental mapping of the globular oxides of various sizes located in the FZ of TRIP steel

A more detailed elemental mapping in **Figure 5** confirms a complex character of the investigated inclusion. Moreover, the small amount of titanium addition was identified. Grajcar et al. [15] observed high amount of complex, oxide-type inclusions in the fusion zone of laser-welded TRIP steel too. Moreover, it was found [17] that the use of protecting gas atmosphere during laser welding had a beneficial effect on reduction of non-metallic inclusions (to a limited extent). Intense evaporation of gases and metal steams destroys partially a protective atmosphere of argon; as a result some oxidation of the weld pool takes place. The non-metallic inclusion located in the martensite laths of CP steel (**Figure 6**) consists of oxygen, carbon, titanium, small amount of aluminium, manganese and silicon (**Figure 6b**). The diameter of the non-metallic inclusion in CP steel is significant lower when compared to TRIP steel.

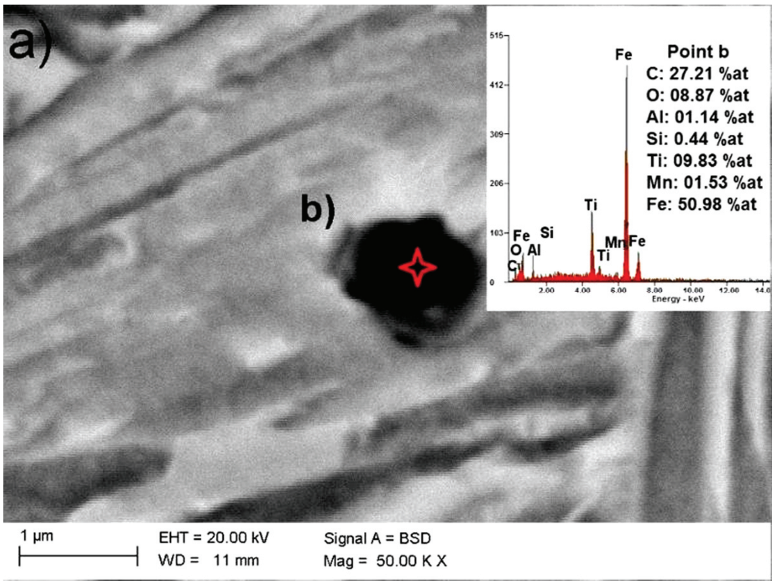

Figure 6 Non-metallic inclusion detected in the fusion zone of CP steel (a); EDS analysis of particle from point marked as b (b)

4. CONCLUSIONS

The lack of protective atmosphere influences a type of non-metallic inclusions formed in the fusion zone of TRIP and CP laser-welded joints. The quantity and size of particles present in FZ of TRIP steel were significantly larger in comparison to CP steel. It is mainly due to the higher content of Al in the TRIP steel. Complex oxide particles containing Mn, Al, Si and Ti were detected in the TRIP steel. A large content of Ti in the CP steel results in the presence of complex carbo-oxides containing a high concentration of Ti.

REFERENCES

[1] KUC, D., HADASIK, E., NIEWIELSKI, G., SCHINDLER, I., MAZANCOVA, E., RUSZ, S., KAWULOK, P. Structural and mechanical properties of laboratory rolled steels high-alloyed with manganese and aluminium. Archives of Civil and Mechanical Engineering, 2012, vol. 12, pp. 312-317.

[2] RADWANSKI, K., WROZYNA, A., KUZIAK, R. Role of the advanced microstructures characterization in modeling of mechanical properties of AHSS steels. Materials Science and Engineering A, 2015, vol. 639, pp. 567-574.

[3] DOBRZANSKI, L.A., CZAJA, M., BOREK, W., LABISZ, K., TANSKI, T. Influence of hot-working conditions on a structure of X11MnSiAl17-1-3 steel for automotive industry. International Journal of Materials and Product Technology, 2015, vol. 51, pp. 264-280.

[4] JIRKOVA, H., KUCEROVA, L., AISMAN, D., MASEK, B. Optimization of the Q-P process parameters for low alloyed steels with 0.2% C. Archives of Metallurgy and Materials, 2014, vol. 59, p. 1205-1210.

[5] EL MEHTEDI, M., SPINARELLI, S., ZRNIK, J. Effect of thermomechanical processing on the microstructure of Si-Mn TRIP steel. Metallurgia Italiana, 2010, vol. 10, pp. 5-10.

[6] SKUBISZ, P., SIŃCZAK, J., SKOWRONEK, T., RUMINSKI, M. Selection of direct cooling conditions for automotive lever made of microalloyed steel. Archives of Civil and Mechanical Engineering, 2012, vol. 12, pp. 418-426.

[7] OZGOWICZ, W., LABISZ, K. Analysis of the state of the fine-dispersive precipitations in the structure of high strength steel Weldox 1300 by means of electron diffraction. Journal of Iron and Steel Research International, 2011, vol. 18, pp. 135-142.

[8] OPIELA, M. Thermodynamic analysis of the precipitation of carbonitrides in microalloyed steels. Materiali in Tehnologije, 2015, vol. 49, pp. 395-401.

[9] SKOLEK, E., MARCINIAK, S., SKOCZYLAS, S., KAMINSKI, J., SWIATNICKI, W.A. Nanocrystalline steels' resistance to hydrogen embrittlement. Archives of Metallurgy and Materials, 2015, vol. 60, pp. 491-497.

[10] MAZANCOVA, E., OSTROUSHKO, D., SAKSL, K., NIESLONY, A. Joint hydrogen susceptibility of 304 SS welded with titanium. Archives of Metallurgy and Materials, 2014, vol. 59, pp. 1605-1610.

[11] LISIECKI, A. Welding of thermomechanically rolled fine-grain steel by different types of lasers. Archives of Metallurgy and Materials, 2014, vol. 59, pp. 1625-1631.

[12] LISIECKI, A., BURDZIK, R., SIWIEC, G., KONIECZNY, L., WARCZEK, J., FOLEGA, P., OLEKSIAK, B. Disc laser welding of car body zinc coated steel sheets. Archives of Metallurgy and Materials, 2015, vol. 60, pp. 2913-2922.

[13] JANICKI, D. Disc laser welding of armor steel. Archives of Metallurgy and Materials, 2014, vol. 59, pp. 1641-1646.

[14] WEGLOWSKI, M.S., ZEMAN, M. Prevention of cold cracking in ultra-high strength steel Weldox 1300. Archives of Civil and Mechanical Engineering, 2014, vol. 14, pp. 417-424.

[15] GRAJCAR, A., ROZANSKI, M., STANO, S., KOWALSKI, A., GRZEGORCZYK, B. Effect of heat input on microstructure and hardness distribution of laser welded Si-Al TRIP-type steel. Advances in Materials Science and Engineering, 2014, vol. 2014, 8 pages, doi.org/10.1155/2014/658947.

[16] GORKA, J. Study of structural changes in S700MC steel thermomechanically treated under the influence of simulated welding thermal cycles. Indian Journal of Engineering and Materials Sciences, 2015, vol. 22, pp. 497-502.

[17] GRAJCAR, A., ROZANSKI, M., KAMINSKA, M., GRZEGORCZYK, B. Effect of gas atmosphere on non-metallic inclusions in laser-welded TRIP steel with Al and Si additions. Materiali in Tehnologije, 2016, vol. 50, (in press).